Immunodeficiency and EBV-induced lymphoproliferation caused by 4-1BB deficiency

Mohammed F. Alosaimi, MD,[a,b] Manfred Hoenig, MD,[c] Faris Jaber, MD,[a] Craig D. Platt, MD, PhD,[a] Jennifer Jones, BA,[a] Jacqueline Wallace, BSPH,[a] Klaus-Michael Debatin, MD,[c] Ansgar Schulz, MD,[c] Eva Jacobsen, PhD,[c] Peter Möller, MD,[d] Hanan E. Shamseldin, MSc,[e] Ferdous Abdulwahab, MSc,[e] Niema Ibrahim, MD,[e] Hosam Alardati, MD,[f] Faisal Almuhizi, MD,[g] Ibraheem F. Abosoudah, MD,[h] Talal A. Basha, MD,[i] Janet Chou, MD,[a]* Fowzan S. Alkuraya, MD,[e]* and Raif S. Geha, MD[a]*

Boston, Mass, Riyadh and Jeddah, Saudi Arabia, and Ulm, Germany

Background: The tumor TNF receptor family member 4-1BB (CD137) is encoded by *TNFRSF9* and expressed on activated T cells. 4-1BB provides a costimulatory signal that enhances CD8$^+$ T-cell survival, cytotoxicity, and mitochondrial activity, thereby promoting immunity against viruses and tumors. The ligand for 4-1BB is expressed on antigen-presenting cells and EBV-transformed B cells.

Objective: We investigated the genetic basis of recurrent sinopulmonary infections, persistent EBV viremia, and EBV-induced lymphoproliferation in 2 unrelated patients.

Methods: Whole-exome sequencing, immunoblotting, immunophenotyping, and *in vitro* assays of lymphocyte and mitochondrial function were performed.

Results: The 2 patients shared a homozygous G109S missense mutation in 4-1BB that abolished protein expression and ligand binding. The patients' CD8$^+$ T cells had reduced proliferation, impaired expression of IFN-γ and perforin, and diminished cytotoxicity against allogeneic and HLA-matched EBV-B cells. Mitochondrial biogenesis, membrane potential, and function were significantly reduced in the patients' activated T cells. An inhibitory antibody against 4-1BB recapitulated the patients' defective CD8$^+$ T-cell activation and cytotoxicity against EBV-infected B cells *in vitro*.

Conclusion: This novel immunodeficiency demonstrates the critical role of 4-1BB costimulation in host immunity against EBV infection. (J Allergy Clin Immunol 2019;■■■:■■■-■■■.)

Key words: *4-1BB, CD137, immunodeficiency, EBV, Hodgkin lymphoma*

EBV is a common infectious pathogen with a strong tropism for B lymphocytes.[1] In immunocompetent hosts primary EBV infection is often asymptomatic or a self-limited disease. In contrast, a subset of immunodeficient patients are susceptible to persistent EBV viremia associated with fever, lymphadenopathy, hepatitis, and pneumonia.[2] Complications of EBV infection in immunodeficient patients include uncontrolled B-cell proliferation, hemophagocytic lymphohistiocytosis, and malignancies.[2]

EBV-specific immunity depends on virus-specific cellular and humoral immunity. The importance of CD8$^+$ cytotoxic T cells in the control of EBV infection is demonstrated by the susceptibility of patients with mutations in genes critical for T-cell development and function to chronic EBV infection.[3] These include defects in genes associated with severe combined immunodeficiencies: *MAGT1*, an Mg^{+2} transporter involved in T-cell receptor and NKG2D signaling; *SH2D1A*, which encodes the SLAM-associated protein; *ITK*, which encodes IL-2–inducible T-cell kinase; and *PFR1*, which encodes perforin 1.[4] Mutations in the T-cell costimulatory TNF family member receptor CD27 and its ligand, the TNF receptor (TNFR) family member CD70, predominantly expressed on B cells, result in impaired generation of IFN-γ– and perforin-producing CD8$^+$ cytotoxic T cells.[5,6] T-cell activation and EBV-specific CD8$^+$ T-cell expansion and cytotoxicity are impaired in CD70-deficient patients.[7,8]

4-1BB is a type II transmembrane protein of the TNFR family expressed as a trimer on the surfaces of activated T cells.[9] 4-1BB has 4 cysteine-rich domains (CRDs) in its extracellular region, of which the CRD2 and CRD3 domains comprise the ligand-binding domain. The intracellular region of 4-1BB interacts with TNFR-associated factor 2.[10] The ligand for 4-1BB (4-1BBL [CD137L]) is a member of the TNF family expressed as a trimer on the surfaces of activated T cells, B cells, dendritic cells, and natural killer (NK) cells.[11-14] Notably, the EBV-encoded latent membrane protein 1 upregulates 4-1BBL expression on B cells.[15] 4-1BB ligation enhances activation of both human CD4$^+$ and CD8$^+$ T cells but preferentially promotes expansion and increased survival of CD8$^+$ T cells. Activation of 4-1BB enhances production of IFN-γ and perforin and mitochondrial biogenesis, contributing to the cytolytic activity of CD8$^+$ T cells.[16-20] The contribution of 4-1BB to CD8$^+$ T-cell function is further demonstrated by decreased IFN-γ production and cytolytic CD8$^+$ T-cell effector function in 4-1BB–deficient mice.[21] The effect of 4-1BB stimulation on cytolytic T-cell responses has been used to increase the potency of vaccines against cancers.[22,23] Additionally,

From [a]the Division of Immunology, Boston Children's Hospital, and the Department of Pediatrics, Harvard Medical School, Boston; [b]the Department of Pediatrics, King Saud University, Riyadh; [c]the Department of Pediatrics and Adolescent Medicine, University Medical Center Ulm; [d]the Institute of Pathology, University of Ulm; [e]the Department of Genetics, King Faisal Specialist Hospital and Research Center, Riyadh; [f]the Department of Pathology and Laboratory Medicine, [h]the Department of Oncology, and [i]the Department of Pediatrics, King Faisal Specialist Hospital and Research Center, Jeddah; and [g]the Department of Medicine, Security Force Hospital, Riyadh.

*These authors contributed equally to this work.

Supported by National Institutes of Health grants 5K08AI116979-04 (to J.C.) and 1R01AI139633-01 (to R.S.G.) and the Perkin Fund (to R.S.G.). This work was supported in part by King Salman Center for Disability Research and the Saudi Human Genome Program.

Disclosure of potential conflict of interest: The authors declare that they have no relevant conflicts of interest.

Received for publication January 14, 2019; revised February 11, 2019; accepted for publication March 1, 2019.

Corresponding author: Raif S. Geha, MD, Division of Immunology, Boston Children's Hospital, 1 Blackfan Circle, Karp Building 10th floor, Boston, MA 02115. E-mail: raif.geha@childrens.harvard.edu.

0091-6749/$36.00

https://doi.org/10.1016/j.jaci.2019.03.002

Abbreviations used
APC: Allophycocyanin
4-1BBL: 4-1BB ligand
CRD: Cysteine-rich domain
E/T: Effector/target
FITC: Fluorescein isothiocyanate
NK: Natural killer
OCR: Oxygen consumption rate
PE: Phycoerythrin
ROH: Region of homozygosity
SNP: Single nucleotide polymorphism
TNFR: TNF receptor

incorporation of the intracellular domain of 4-1BB in the architecture of chimeric antigen receptors increases the cytotoxicity of chimeric antigen receptor T cells against tumor targets.[24,25]

We present 2 unrelated patients with sinopulmonary infections, chronic EBV viremia, and EBV-driven lymphoproliferation. The patients shared a homozygous G109S missense mutation in 4-1BB that abolished 4-1BB surface expression and ligand binding. The patients' $CD8^+$ T cells demonstrated reduced proliferation, impaired expression of IFN-γ and perforin, and diminished cytotoxicity against allogeneic and HLA-matched EBV-transformed B cells. Addition of an inhibitory 4-1BB antibody to cultures of normal PBMCs stimulated with allogeneic or autologous EBV-B cells recapitulated the patients' $CD8^+$ T-cell functional defects. These results support a critical role for 4-1BB in host immunity against EBV infection.

METHODS

Patients

All study participants provided written informed consent approved by the respective institutional review boards of the referring hospitals.

Genetic studies

Genomic DNA was genotyped by using a genome-wide single nucleotide polymorphism (SNP) array (Axiom SNP chip; Affymetrix, Santa Clara, Calif). Genotype files were analyzed by using AutoSNPa software (http://dna.leeds.ac.uk/autosnpa/) to search for shared regions of homozygosity (ROHs), followed by in-depth analysis of the underlying haplotypes. Exome sequencing was performed, as described previously.[26] Variants were prioritized based on residing within the candidate autozygous interval, being coding/splicing variants, and being novel or very rare (minor allele frequency < 0.0001) in public databases (gnomAD) and our database of 2379 ethnically matched in-house exomes, as previously described.[27] Sanger sequencing was used to validate the identified mutation in the probands and verify the carrier status of the parents.

Immunophenotyping

Conjugated mAbs used for flow cytometric studies of T and B cells were as follows: anti-CD45RA–allophycocyanin (APC)-Cy7, anti-CD56–phycoerythrin (PE), anti-CD3–fluorescein isothiocyanate (FITC), anti-CD4–BV605, anti-CD8–APC, and anti-CCR7–BV421 (all from BioLegend, San Diego, Calif).

T-cell proliferation

T-cell proliferation was measured by adding 1 μCi of tritiated thymidine for 16 hours after stimulation with immobilized anti-CD3 (3 μg/mL; OKT3; eBioscience, San Diego, Calif) and anti-CD28 (1 μg/mL; eBioscience) or PHA (4 μg/mL; Sigma-Aldrich, St Louis, Mo), as previously described.[28]

Cytokine secretion

IFN-γ and IL-2 levels were measured in supernatants of PHA-stimulated PBMCs by using a Cytometric Bead Array from BD Biosciences (San Jose, Calif), according to the manufacturer's instructions.

4-1BB and 4-1BBL expression and 4-1BBL binding

Unstimulated and PHA (4 μg/mL)–stimulated PBMCs (5×10^5) were stained on ice for 30 minutes with anti–4-1BB–PE, anti–4-1BBL–APC, anti-CD4–BV605, anti-CD8–FITC, and anti-CD25–BV421 (all from BioLegend). For 4-1BBL binding, PBMCs were incubated first with chimeric CD137L:muCD8 fusion protein (Axxora ANC-503) and then washed and incubated with murine anti-CD8–PE.

Immunoblotting

Lysates from PHA (4 μg/mL)–stimulated PBMCs in RIPA buffer (Millipore, Temecula, Calif) and protease inhibitors (Sigma-Aldrich offers Roche, Mannheim, Germany) were electrophoresed on 4-12% precast polyacrylamide gels (Bio-Rad Laboratories, Hercules, Calif), followed by immunoblotting with polyclonal rabbit antibody against the intracellular region of 4-1BB (LS-C135872). Anti–β-actin antibody was used as a control (Cell Signaling, Danvers, Mass).

Intracellular cytokine staining

PBMCs (5×10^5) were incubated with phorbol 12-myristate 13-acetate (5 ng/mL), ionomycin (500 ng/mL), Brefeldin A, and monensin for 4 hours and then fixed and permeabilized with BD Cytofix/Cytoperm. Cells were then incubated overnight on ice with anti–IFN-γ–APC, anti-perforin–PE, and anti-CD8–FITC (all from BioLegend). Analyses were performed with FlowJo software (TreeStar, Ashland, Ore).

Cytotoxic T-cell generation and killing assay

EBV-transformed B-cell lines were generated, as previously described.[29] PBMCs were stimulated with mitomycin C–treated autologous or allogeneic EBV-lymphoblastoid cell lines in the presence of IL-7 (10 ng/mL; PeproTech, Rocky Hill, NJ). 4-1BB blocking antibody (clone BBK-2-azide free; LifeSpan BioScienes, Seattle, Wash) was added every 7 days to control PBMC cultures. Three rounds of stimulation were performed at 7-day intervals. IL-2 (100 U/mL) was added on day 14 of culture. A responder/stimulator ratio of 10:1 was used throughout the rounds of stimulation. At day 21, $CD8^+$ T cells were isolated by means of negative selection using the $CD8^+$ T Cell Isolation Kit from Miltenyi Biotec (Bergisch Gladbach, Germany), according to the manufacturer's protocol. $CD8^+$ T cells were incubated for 4 hours with live EBV-B cell targets at different effector/target (E/T) cell ratios, and cytotoxicity was measured by means of flow cytometry gating on $CD19^+$ and by using Annexin V and fixable viability dye (Thermo Fisher Scientific, Waltham, Mass), as previously described.[30] The cytotoxicity percentage was measured as 100 minus the percentage of Annexin V– and fixable viability dye–negative EBV cells.

Oxygen consumption

Oxygen consumption rates (OCRs) were measured with the Seahorse XFp Analyzer (Agilent Technologies, Santa Clara, Calif). T lymphocytes (1×10^5) purified from PHA-stimulated PBMC cultures for 3 days were plated per each well in Seahorse XF base medium with 2 mmol/L glutamine, 10 mmol/L glucose, and 2.5 mmol/L pyruvate. OCRs were measured at baseline and in the presence of 1 μmol/L oligomycin, 4 μmol/L carbonyl cyanide-4(trifluoromethoxy) phenylhydrazone, and 0.5 μmol/L antimycin A/rotenone.

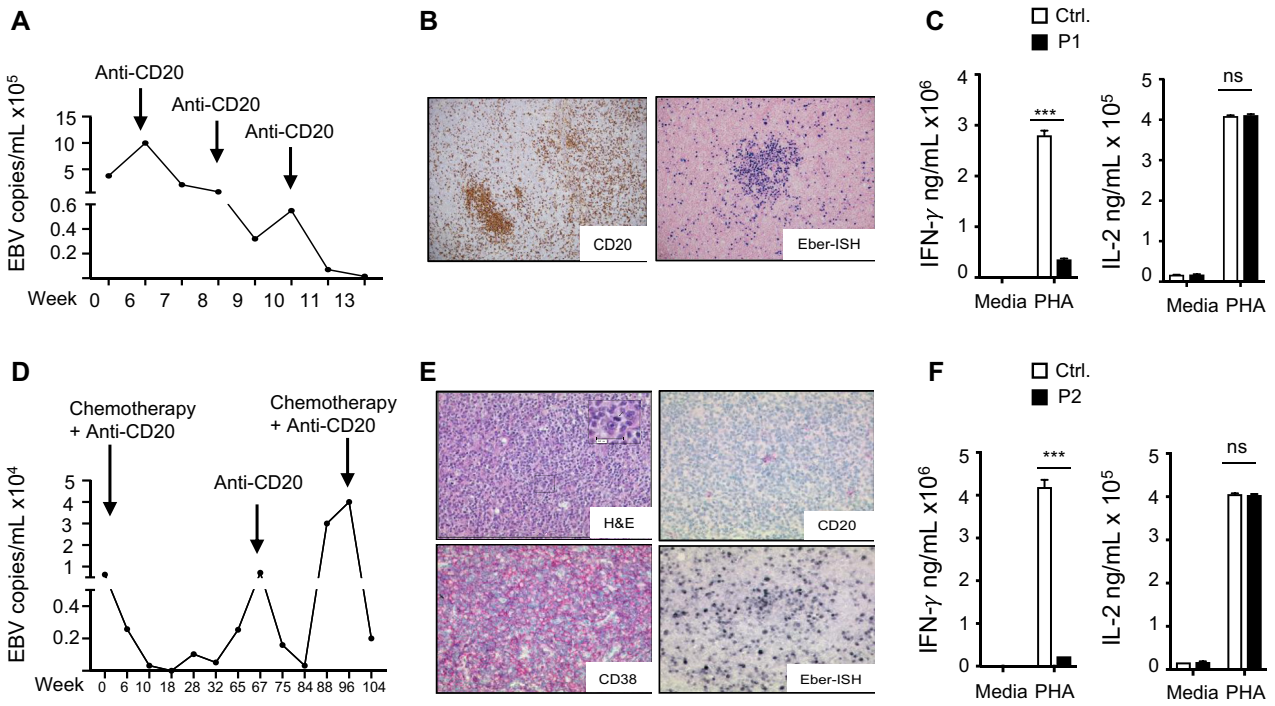

FIG 1. EBV viremia, EBV-driven lymphoproliferation, and impaired IFN-γ secretion in the patients. **A,** Circulating EBV viral load in patient 1. **B,** Immunohistochemistry of cervical lymph nodes from patient 1 showing a cluster of $CD20^+$ B cells *(left)* and positive EBV *(EBER) in situ* hybridization *(right)*. **C,** IFN-γ and IL-2 levels in supernatants of PHA-stimulated PBMCs from patient 1 and control subjects (n = 3) in 2 independent experiments. **D,** Circulating EBV viral load in patient 2. **E,** Hematoxylin and eosin *(H&E)* stain of cervical lymph nodes from patient 2 showing a diffuse growth pattern *(upper left)* and immunohistochemistry showing negative CD20 staining *(upper right)*, positive CD38 staining *(lower left)*, and positive EBV *(EBER)* in *situ* hybridization *(lower right)* consistent with a diffuse large B-cell lymphoma of the plasmablastic subtype. **F,** IFN-γ and IL-2 levels in supernatants of PHA-stimulated PBMCs from patient 2 and control subjects (n = 3) in 2 independent experiments. Results represent means, and *columns* and *bars* represent means + SEMs. ***$P < .001$. *ns*, Not significant.

Mitochondrial studies

Unstimulated and PHA (4 μg/mL)–stimulated PBMCs (5×10^5) were stained at 37°C for 25 minutes with MitoTracker Green (100 nmol/L) and MitoTracker Red CMXRos (200 nmol/L). Cells were washed with warm PBS and immediately analyzed without fixation. Mitochondrial stains were from Thermo Fisher.

Statistics

Statistical analysis was performed by using GraphPad Prism software (GraphPad Software, La Jolla, Calif). The Student *t* test was used for comparisons of 2 groups; unless otherwise indicated, 1-way ANOVA was used for comparison of more than 2 groups, with the Holm-Šídák postcomparison test. Data are graphed as means with SEMs.

RESULTS

Two patients with immunodeficiency and EBV lymphoproliferation

We studied 2 Saudi patients who were products of first-cousin marriages but not known to be related. Patient 1 presented at 3 years of age with sinopulmonary infections, bronchiectasis, and an episode of pneumococcal septicemia. Her sinopulmonary infections improved with intravenous gammaglobulin replacement therapy. At 5 years of age, she had generalized lymphadenopathy and was found to have EBV viremia (Fig 1, *A*). Cervical lymph node biopsy showed multiple clusters of $CD20^+$ B cells (Fig 1, *B*). Results of *in situ* hybridization were positive for EBV-encoded RNA (Fig 1, *B*).

Laboratory evaluation at that time revealed normal numbers of T, B, and NK cells; hypogammaglobulinemia (IgG, 440 mg/dL [normal range, 500-1490 mg/dL]; IgM, 318 mg/dL [normal range, 37-224 mg/dL]; and IgA, <45 mg/dL [normal range, 29-256 mg/dL]); poor antibody response to tetanus toxoid (0.2 IU/mL [normal range, >0.4 IU/mL]); and undetectable antibody titers to pneumococcal polysaccharide vaccine (Pnumovax-23), which the patient has received (normal range, >3.3 ug/mL). She subsequently had hemophagocytic lymphohistiocytosis with persistent fevers, splenomegaly, pancytopenia, increased serum levels of triglycerides (345 mg/dL [normal, <150 mg/dL]) and soluble CD25 (>5000 pg/mL [normal, 450-1997 pg/mL]), and low serum levels of fibrinogen (140 mg/dL [normal, >150 mg/dL]). She was treated with anti-CD20 mAb (rituximab), leading to resolution of her viremia (Fig 1, *A*). After rituximab treatment, she was found to have increased percentages of effector memory T cells, undetectable B cells, and decreased proliferation to PHA and anti-CD3 plus anti-CD28 stimulation (Table I). PHA-driven IFN-γ secretion by PBMCs was significantly reduced, but IL-2 secretion was normal (Fig 1, *C*). She is currently undergoing hematopoietic stem cell transplantation from a healthy HLA-matched sibling.

TABLE I. Immunologic profiles of the patients

Hemogram (normal range)	Patient 1, 5 y (after rituximab)	Patient 2, 9 y (after chemotherapy)
Hemoglobin (g/dL)	11.3 (10.5-13.8)	11.8 (11.9-14.7)
WBCs (10^3 cells/μL)	10.4 (5.4-9.7)	3.1 (4.4-9.1)
Neutrophils (10^3 cells/μL)	2.39 (1.5-5.9)	1.4 (1.8-8.0)
Lymphocytes, (10^3 cells/μL)	6.81 (1.28-2.76)	0.96 (1.9-3.7)
Monocytes (10^3 cells/μL)	0.65 (0.19-0.81)	0.6 (<0.8)
Platelets (10^3 cells/μL)	412 (187-450)	196 (247-436)
Lymphocyte subsets (normal range)		
$CD3^+$ (cells/μL)	3,352 (770-4,000)	807 (1,200-2,600)
$CD3^+CD4^+$ (cells/μL)	2,766 (400-2,500)	365 (650-1,500)
$CD45RA^+CCR7^+$ (% $CD4^+$ [naive])	23.9 (57.1-84.8)	8 (57.1-84.8)
$CD45RA^+CCR7^-$ (% CD4+ [Temra])	1.18 (0.4-2.6)	0.7 (0.4-2.6)
$CD45RA^-CCR7^+$ (% $CD4^+$ [CM])	9.8 (11.2-26.7)	22.3 (11.2-26.7)
$CD45RA^-CCR7^-$ (% $CD4^+$ [EM])	65.1 (3.3-15.2)	69.7 (3.3-15.2)
$CD3^+CD8^+$ (cells/μL)	627 (490-1,300)	413 (370-1,100)
$CD45RA^+CCR7^+$ (% $CD8^+$ [naive])	42.4 (28.4-80)	17.8 (28.4-80)
$CD45RA^+CCR7^-$ (% $CD8^+$ [Temra])	7.36 (9.1-49.1)	29.8 (9.1-49.1)
$CD45RA^-CCR7^+$ (% $CD8^+$ [CM])	0.7 (1-4.5)	3.5 (1-4.5)
$CD45RA^-CCR7^-$ (% $CD8^+$ [EM])	49.6 (6.2-29.3)	48.9 (6.2-29.3)
$CD19^+$ (cells/μL)	0 (390-1,400)	0 (270-860)
$CD3^-CD56^+$ (cells/μL)	114 (110-720)	144 (80-600)
Proliferation CPM (normal control)		
PHA	64,562 (113,646)	56,218 (111,191)
Anti-CD3 plus anti-CD28	20.650 (78,008)	35,638 (72,876)
Media	1,905 (1,504)	195 (145)

CM, Central memory; *EM*, effector memory; *ND*, not done; *Temra*, exhausted.

Patient 2 presented at 6 years of age with recurrent sinopulmonary infections, generalized lymphadenopathy, splenomegaly, and EBV viremia (Fig 1, *D*). He had increased serum levels of IgG (4898 mg/dL [normal range, 34-274 mg/dL]) and IgA (272 mg/dL [normal range, 25-154 mg/dL]) but low levels of IgM (25 mg/dL [normal range, 38-251 mg/dL]). He received a diagnosis of EBV-positive Hodgkin disease.

The patient received 5 cycles of chemotherapy in the form of doxorubicin, bleomycin, vincristine, etoposide, prednisone and cyclophosphamide along with rituximab. Chemotherapy and rituximab treatment resulted in clinical remission and resolution of the viremia. Intravenous gammaglobulin replacement therapy improved his respiratory tract infections. Subsequently, he was found to have decreased numbers of T cells with increased percentages of effector memory T cells, undetectable B cells, and reduced proliferation to PHA and anti-CD3 plus anti-CD28 stimulation. PHA-driven IFN-γ secretion by PBMCs was significantly reduced, but IL-2 secretion was normal (Fig 1, *F*), as observed in patient 1. He relapsed 1 year later with recurrence of lymphoma and EBV viremia (Fig 1, *D*). Lymph node biopsy showed a progression to a diffuse large B-cell lymphoma negative for CD20 and positive for CD38 expression (Fig 1, *E*). Results of *in situ* hybridization were positive for EBV-encoded RNA (Fig 1, *E*). He received daratumumab (anti-CD34 mAb), bortezomib, dexamethasone, and rituximab (anti-CD20 mAb). This resulted in clinical improvement and resolution of the viremia. Patient 2 has no HLA-matched siblings.

A homozygous 4-1BB^{G109S} mutation in the patients abolishes 4-1BB expression. Homozygosity analysis of SNP array results revealed that the 2 patients shared 1 ROH that comprised an identical founder haplotype (chromosome 1: 7186325-8273940; delimited by SNPs rs4460663-rs395847). Although the patients' families are not known to be related, the shared interval suggests a founder effect. Whole-exome sequencing revealed only 2 novel homozygous variants within this candidate locus: *CAMTA1* and *TNFRSF9*. The *CAMTA1* variant (NM_015215.3:c.2370C>G: p.Ile790Met) affected a poorly conserved residue and was considered unlikely because the gene has an established link to autosomal dominant cerebellar ataxia with mental retardation, a phenotype irrelevant to the patient. The shared *TNFRSF9* variant (NM_001561:c.325G>A: p.Gly109Ser) was absent in gnomAD and in our database of 2379 ethnically matched in-house exomes. The *TNFRSF9* variant was predicted to be pathogenic by using the PolyPhen (0.999), SIFT (0.03), and CADD.[30] Sanger sequencing revealed that the mutation is homozygous in both patients (Fig 2, *A*) and heterozygous in their parents (data not shown).

Table E1 in this article's Online Repository at www.jacionline.org lists all the variants shared by both probands with a minor allele frequency of less than 0.001 in gnomAD. No exonic mutations in any of the genes known to be associated with immunodeficiency and EBV-driven B-cell lymphoproliferation were detected.

The mutated G109 residue in 4-1BB is highly conserved (Fig 2, *B*). It resides in the third CRD of the extracellular region of 4-1BB but does not directly interact with the 4-1BB ligand 4-1BBL (Fig 2, *C* and *D*). Modeling based on the crystal structure of the 4-1BB/4-1BBL complex[9] suggests that the mutated S109 residue could form hydrogen bonds with nearby polar residues, altering the protein's folding, structure, or stability (Fig 2, *D*).

4-1BB is expressed on T cells only after activation.[17] Immunoblotting with a polyclonal rabbit antibody directed against the intracellular domain of 4-1BB (residues 214-255) revealed 4-1BB expression in lysates from PHA-activated PBMCs from healthy control subjects but not from the 2 patients (Fig 2, *E*), indicating that the mutant protein is not expressed. PHA

stimulation induced 4-1BB surface expression on $CD8^+$ and $CD4^+$ cells from control subjects but not from the 2 patients (Fig 2, *F*, and see Fig E1, *A*, in this article's Online Repository at www.jacionline.org). Furthermore, recombinant 4-1BBL bound PHA-activated $CD8^+$ and $CD4^+$ T cells from control subjects but not from the patients (Fig 2, *E*, and see Fig E1, *A*). The absence of 4-1BB expression and 4-1BBL binding by patients' T cells was not secondary to poor T-cell activation because the patients' $CD8^+$ and $CD4^+$ T cells robustly upregulated CD25 surface expression after PHA activation (Fig 2, *E*, and see Fig E1, *A*). Consistent with lack of expression of the mutant protein, PHA-activated $CD4^+$ and $CD8^+$ T cells from the heterozygous parents of the patients demonstrated an approximately 50% reduction in 4-1BB expression (see Fig E1, *B*).

Defective expansion, reduced expression of IFN-γ and perforin, and impaired allospecific and EBV-specific cytotoxic activity of patients' $CD8^+$ T cells

4-1BB costimulation promotes $CD8^+$ T-cell expansion, IFN-γ and perforin secretion, and cytotoxic activity.[16-18,31] PBMCs were stimulated in 3 consecutive 1-week rounds with mitomycin C–treated allogeneic EBV B cells from a non–HLA-matched donor to determine the effect of the $4\text{-}1BB^{G109S}$ mutation on the generation and function of cytotoxic $CD8^+$ T cells (Fig 3, *A*). In these cocultures EBV-B cells express 4-1BBL, and activated $CD8^+$ T cells express 4-1BB (see Fig E2 in this article's Online Repository at www.jacionline.org). After the second and third rounds of stimulation (days 14 and 21), aliquots of cells were analyzed for $CD8^+$ T-cell numbers and intracellular expression of IFN-γ and perforin (Fig 3, *A*). Stimulation with allogeneic EBV-B cells caused progressive expansion and intracellular expression of IFN-γ and perforin in control $CD8^+$ T cells (Fig 3, *B* and *C*). In contrast, the patients' $CD8^+$ T cells had significantly less expansion compared with control subjects and reduced expression of IFN-γ and perforin (Fig 3, *B* and *C*). After 3 rounds of stimulation, control $CD8^+$ T cells purified from normal cultured PBMCs stimulated with allogeneic EBV cells exhibited robust cytotoxicity against the priming EBV-B cells (Fig 3, *D*). As expected, they had minimal cytotoxicity against EBV-B cells from a third-party donor, HLA-mismatched with the donor of the EBV-B cell line used for stimulation (<5% killing at an E/T cell ratio of 8:1), demonstrating the specificity of EBV-primed cytotoxic $CD8^+$ T cells to the priming donor cells. The cytotoxic activity of the patients' $CD8^+$ T cells against allogeneic EBV-B cells was significantly reduced compared with that of control $CD8^+$ T cells from healthy control subjects (Fig 3, *D*). Importantly, addition of an inhibitory anti–4-1BB antibody to cultures of normal PBMCs stimulated with allogeneic EBV-B cells reduced the expansion, intracellular expression of IFN-γ and perforin, and allocytotoxicity to levels comparable with those of the patients' $CD8^+$ cells (Fig 3, *B-D*). Collectively, these findings demonstrate that 4-1BB deficiency impairs the generation and function of allocytotoxic $CD8^+$ cells.

EBV-specific $CD8^+$ cell cytotoxicity is important for EBV immunity and is typically tested by using autologous EBV-B cells.[2,8] We were unable to generate EBV-transformed B-cell lines from the patients because both had undetectable B cells after rituximab treatment. In lieu of this, we tested the EBV-specific expansion and cytotoxicity of $CD8^+$ cells in cultures of PBMCs from patient 1 against EBV-transformed B cells from her HLA-matched sibling. Expansion and cytotoxicity of $CD8^+$ cells in cultures of PBMCs from a control donor stimulated with autologous EBV-B cells were measured as a positive control. The stimulation protocol was similar to that used to test cytotoxicity against allogeneic EBV-B cells (Fig 3, *A*). Priming of normal PBMCs with autologous EBV-B cells caused $CD8^+$ T cells to expand, express IFN-γ and perforin, and exhibit cytotoxicity against autologous EBV-B cell targets (Fig 3, *E-G*) but not against autologous PHA T-cell blasts (<5% killing at E/T cell ratio of 8:1). $CD8^+$ T-cell expansion, expression of IFN-γ and perforin, and cytotoxicity against HLA-matched EBV-B cell targets were significantly reduced in cultures of PBMCs from patient 1 stimulated with HLA-matched EBV-B cells compared with control cultures stimulated with autologous EBV-B cells (Fig 3, *E-G*). Addition of an inhibitory anti–4-1BB antibody reduced the cytotoxicity of control $CD8^+$ cells against autologous EBV-B cells to a level comparable with that of patients' $CD8^+$ cells against HLA-matched EBV-B cells (Fig 3, *E-G*). Collectively, these data support a critical role for 4-1BB in the expansion and function of EBV-specific $CD8^+$ cells.

Defective mitochondrial biogenesis and function in the patients' activated T cells

In PHA-stimulated PBMC cultures, $CD19^+$ B cells, $CD14^+$ monocytes, and $CD11c^+$ dendritic cells express 4-1BBL, which interacts with 4-1BB expressed on activated T cells (see Fig E3 in this article's Online Repository at www.jacionline.org). 4-1BB ligation enhances mitochondrial biogenesis and increases oxidative phosphorylation in activated T cells.[19,20] We used extracellular flux analysis to measure OCRs in T cells purified from PHA-stimulated PBMC cultures. The combination of protons, electrons, and oxygen in the mitochondrial matrix determines the mitochondrial OCR and reflects mitochondrial function. In the inner mitochondrial membrane, complexes I to IV of the electron transport chain catalyze electron transfers and generate the proton gradient across the inner mitochondrial membrane, which ultimately drives ATP synthesis by complex V. The addition of oligomycin to purified T cells inhibits proton flow through complex V, revealing the basal OCR generated by complexes I to IV (Fig 4, *A*). Carbonyl cyanide-4(trifluoromethoxy) phenylhydrazone permeabilizes the inner mitochondrial membrane, permitting proton entry into the mitochondrial matrix through the concentration gradient, thereby providing the substrate for maximal OCR (Fig 4, *A*). Rotenone and antimycin inhibit complexes I and III, thereby terminating electron transport chain function and abrogating mitochondrial respiration (Fig 4, *A*). Patient 2's T cells showed decreased basal and maximal oxygen consumption (Fig 4, *B*), indicating reduced mitochondrial function activity compared with control subjects. Similarly, the addition of an inhibitor anti–4-1BB antibody to PHA-stimulated control PBMCs reduced baseline and maximal OCRs to a level comparable with those in patients' T cells (Fig 4, *B*).

To further delineate the mechanisms underlying impaired mitochondrial function in the patients' T cells, we measured mitochondrial mass and membrane potential in PHA-activated $CD8^+$ T cells. The mitochondrial mass in the patients' activated $CD8^+$ T cells was significantly reduced compared with that in control subjects (Fig 4, *C*). The mitochondrial membrane potential, which is determined by electric polarization of the inner mitochondrial membrane, is required for oxidative

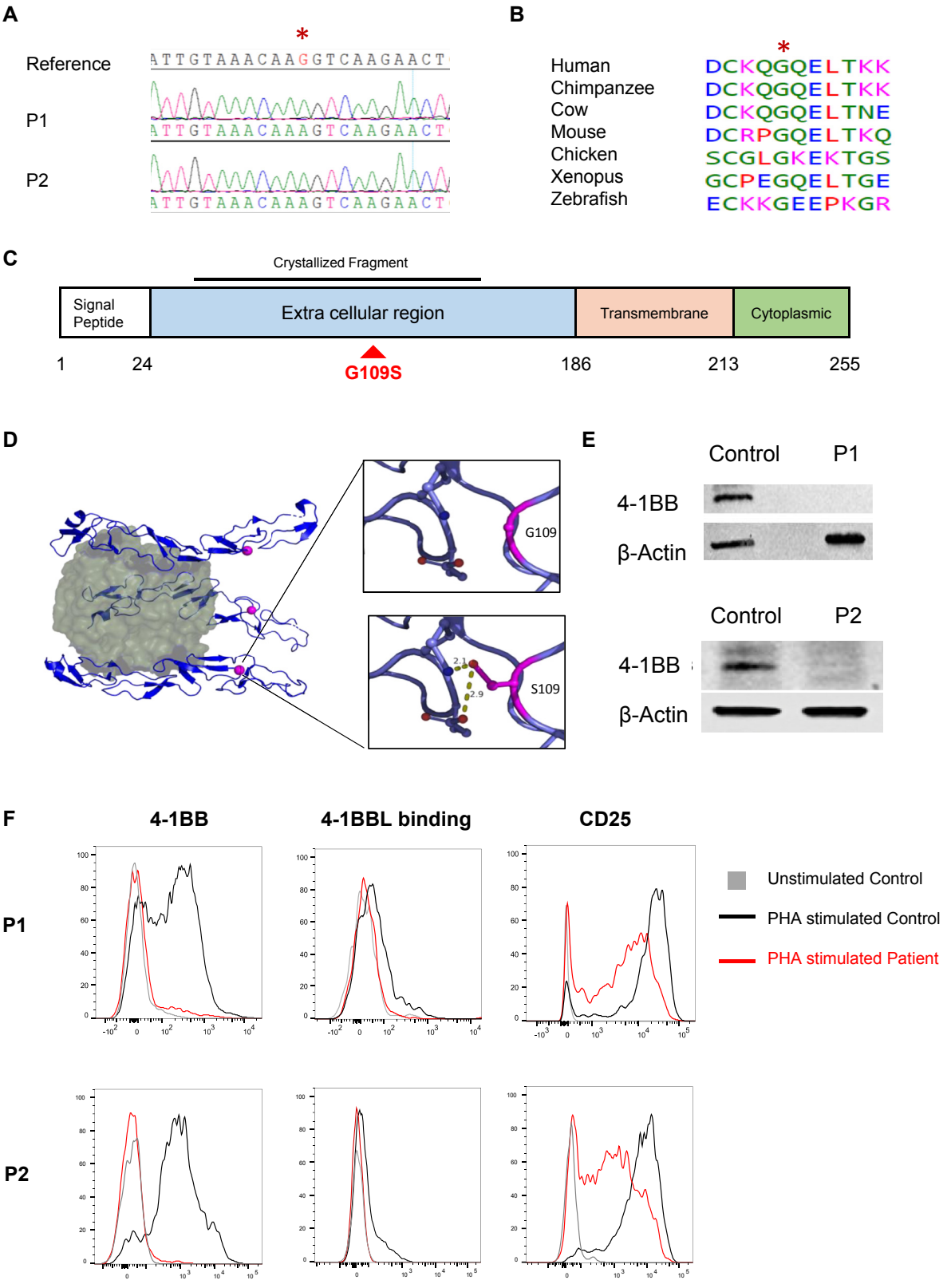

FIG 2. The 4-1BB^{G109S} mutation and its effect on 4-1BB expression. **A,** Sanger sequencing around the missense *TNFRSF9* mutation (c.325G>A: p.Gly109Ser) in a reference control subject and the patients. The mutated nucleotide is indicated in red and by an *asterisk*. **B,** Evolutionary conservation of the S109 amino acid in 4-1BB. Protein sequence orthologous to human 4-1BB was aligned in 6 nonhuman vertebrate species, all of which shared the p.S109 amino acid. **C,** Linear schematic of 4-1BB showing its domains and the location of the G109S mutation (red) in the extracellular domain. The 4-1BB fragment crystallized in

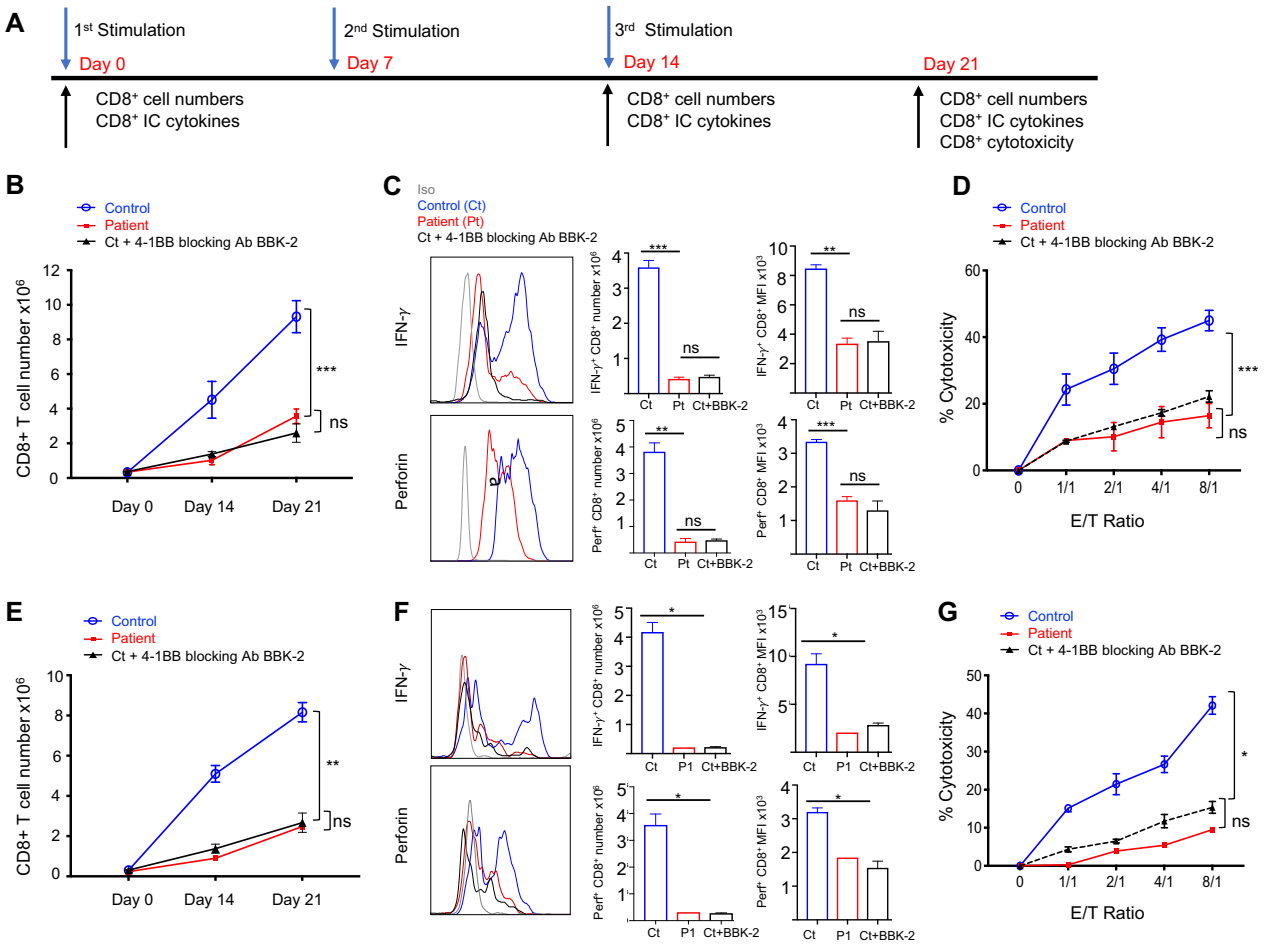

FIG 3. The 4-1BB^{G109S} mutation impairs generation of allospecific and EBV-specific CD8$^+$ T cells. **A,** Experimental protocol for generation and testing of cytotoxic CD8$^+$ T cells against EBV-B cells. *IC*, Intracellular. **B,** CD8$^+$ T-cell numbers on days 0, 14, and 21 after stimulation with allogeneic EBV-B cells of PBMCs from patients (n = 2), control subjects (n = 4), and control subjects with addition of the anti–4-1BB blocking antibody *(Ab)* BBK-2 (n = 2). **C,** Representative fluorescence-activated cell-sorting analysis *(left)*, quantitative analysis *(center)*, and mean fluorescence intensity (*MFI*; *right*) of CD8$^+$IFN-γ$^+$ and CD8$^+$/perforin-positive cells on day 14 after stimulation of PBMCs stimulated with allogeneic EBV-B cells, as described in Fig 3, *B*. **D,** Cytotoxic activity of CD8$^+$ T cells against the stimulatory allogeneic EBV B cells. CD8$^+$ T cells were purified on day 21 from cultures of stimulated PBMCs from patients (n = 2) and control subjects (n = 4). The effect of the anti–4-1BB blocking antibody BBK-2 was examined in 2 of the 4 control subjects (n = 2). **E-G,** CD8$^+$ T-cell numbers (Fig 3, *F*), numbers of CD8$^+$IFN-γ$^+$ and CD8$^+$/perforin-positive cells (Fig 3, *H*), and cytotoxicity of CD8$^+$ T cells (Fig 3, *G*) on day 21 after stimulation of PBMCs from patient 1 with HLA-matched EBV-B cells and normal PBMCs stimulated with autologous EBV-B cells without or with addition of the anti–4-1BB blocking antibody BBK-2 (n = 4 and n = 2, respectively). We were able to study patient 1's CD8$^+$ T-cell cytotoxicity against HLA-matched EBV-B cell targets once because the patient underwent hematopoietic stem cell transplantation. *Symbols* and *bars* in Fig 3, *B*, *D*, *E*, and *G*, and *columns* and *bars* in Fig 3, *C* and *F*, represent means and SEMs. *P < .05, **P < .01, and ***P < .001. *ns*, Not significant.

phosphorylation, mitochondrial structure, and function. The mitochondrial membrane potential of the patients' activated CD8$^+$ T cells was significantly reduced compared with that in control subjects (Fig 4, *D*). Mitochondrial mass and membrane potential were also found to be significantly reduced in PHA-activated CD4$^+$ patients' T cells (see Fig E4 in this article's

complex with 4-1BB (PDB:6PCR) is indicated **D,** Ribbon diagram of the 4-1BB extracellular in complex 4-1BBL. The 4-1B trimer (blue) is shown bound to its trimeric ligand 4-1BBL (green). The *red dot* corresponds to the location of the mutated G109 residue. *Insets* show the potential of the mutated S109 residue to form hydrogen bonds with neighboring polar residues. **E,** Immunoblot analysis of PHA-stimulated PBMCs from both patients and control subjects by using a polyclonal antibody directed against the intracellular domain of 4-1BB. Actin was used as loading control. **F,** Fluorescence-activated cell-sorting analysis of 4-1BB expression *(left)*, 4-1BBL binding *(center)*, and CD25 expression *(right)* in PHA-stimulated CD8$^+$ T cells from the patients and a control subject. Similar results were obtained from 2 independent experiments in Fig 2, *E* and *F*.

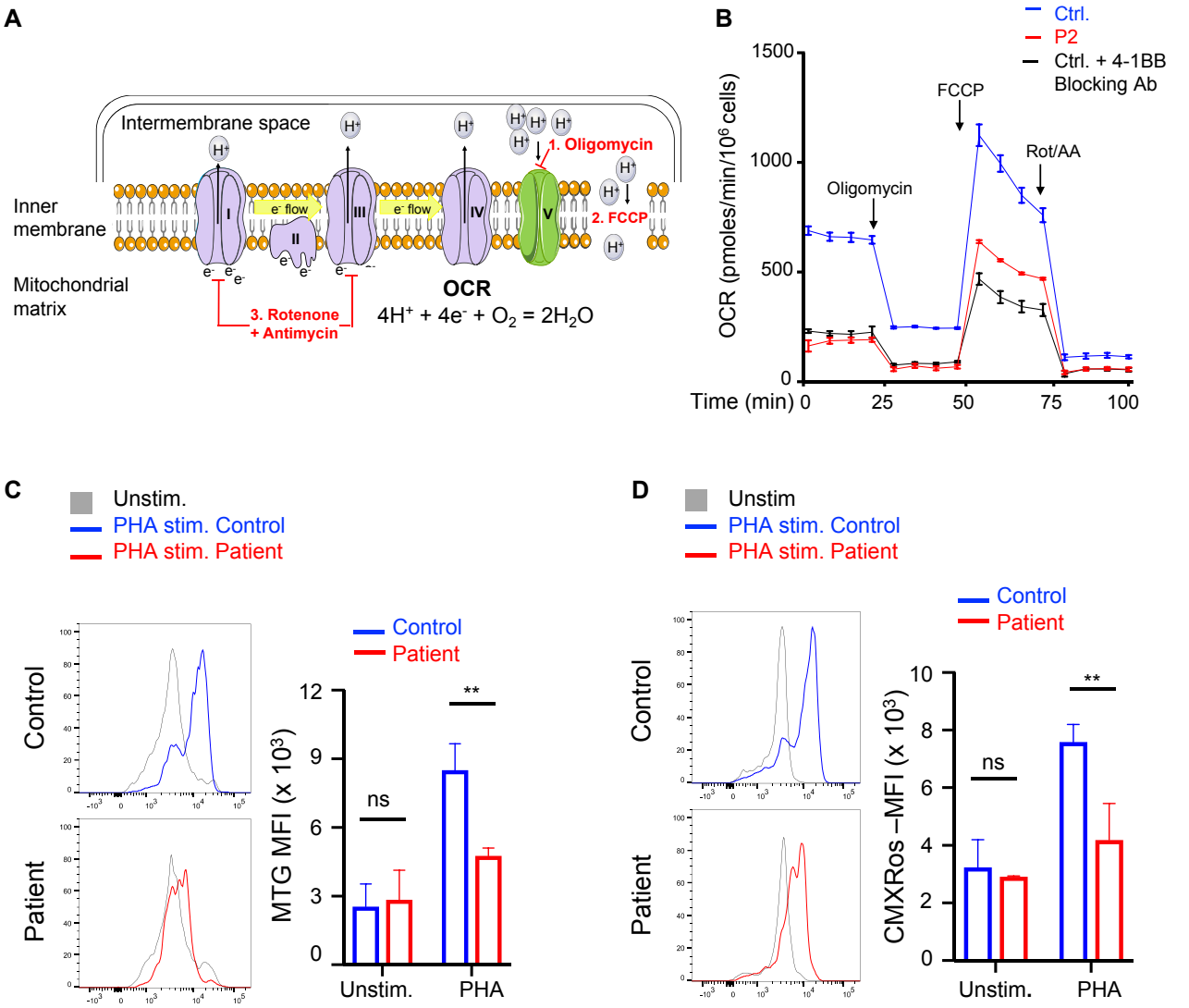

FIG 4. Defective mitochondrial biogenesis and function in patients' activated $CD8^+$ T cells. **A,** Schematic of factors determining OCRs. Complexes I to IV comprise the electron transport chain. The stepwise addition of reagents used during the extracellular flux analysis *(1–3)* is depicted in red. **B,** Extracellular flux analysis of T cells purified from PHA-stimulated PBMCs for 3 days from patient 2 (data are pooled from 2 independent experiments) and control subjects without or with the 4-1BB blocking antibody BBK-2 (n = 2). *FCCP,* Carbonyl cyanide-4(trifluoromethoxy) phenylhydrazone; *ROT/AA,* rotenone/antimycin A. **C** and **D,** Representative fluorescence-activated cell-sorting analysis *(left)* and quantitative analysis (mean fluorescence intensity *[MFI], right*) of mitochondrial mass measured by using MitoTracker Green (*MTG*; Fig 4, *C*) and of mitochondrial membrane potential measured by using MitoTracker Red CMXRos (Fig 4, *D*) of $CD8^+$ cells in PHA-stimulated cultures of PBMCs from patients (n = 2) and control subjects (n = 3). *Columns* and *bars* represent means + SEMs. $^{**}P < .01$. *ns,* Not significant.

Online Repository at www.jacionline.org). Together, these results indicate that 4-1BB deficiency impairs mitochondrial biogenesis and function in activated T cells.

DISCUSSION

We report 2 patients with immunodeficiency and EBV-driven lymphoproliferation caused by a homozygous missense mutation in 4-1BB. 4-1BB protein was not detected on the surfaces of the patients' PHA-activated T cells by using flow cytometry or in their lysates by using immunoblotting with a different antibody. Furthermore, the mutation abolished 4-1BBL binding to activated T cells from the patients. The patients' $CD8^+$ T cells had impaired expansion, reduced expression of IFN-γ and perforin, and defective cytotoxicity against allogeneic EBV cell targets, demonstrating the contribution of 4-1BB to host immunity against EBV.

Both patients had recurrent sinopulmonary infections that improved with gammaglobulin replacement therapy. Patient 1, for whom data were available before treatment with rituximab, had hypogammaglobulinemia and a poor antibody response to tetanus vaccination on presentation. The poor antibody response to tetanus is consistent with the impaired antibody response of 4-1BB–deficient mice to the T cell–dependent antigen keyhole limpet hemocyanin.[21] 4-1BB ligation is known to amplify $CD4^+$

T-cell proliferation and cytokine secretion. PHA-driven IFN-γ secretion was impaired in both patients, whereas IL-2 secretion was intact, suggesting a more stringent requirement for 4-1BB costimulation for IFN-γ secretion by human T cells. The patients' $CD4^+$ T cells demonstrated impaired mitochondrial function, which is indicative of impaired metabolic fitness. Therefore ligation of 4-1BB on $CD4^+$ T_H cells by 4-BBL expressed on antigen-presenting cells and B cells might be important for the optimal response to T cell–dependent antigens.

The mechanism behind the poor antibody response to Pneumovax observed in patient 1 is unknown. In human subjects CD137 signaling promotes B-cell proliferation and survival, as well as secretion of TNF-α,[32] both of which are important for the antibody response to the type II T-independent antigen pneumococcus vaccine.[33] Impaired proliferation and/or insufficient TNF-α secretion by 4-1BB–deficient B cells in response to type II T-independent antigens might underlie the poor antibody response to Pneumovax in patient 1.

Of critical relevance to the EBV viremia and EBV-driven lymphoproliferation, $CD8^+$ T-cell expansion, expression of IFN-γ and perforin, and cytotoxicity against allogeneic EBV-B cells were all severely impaired in both patients. Because an HLA-matched donor has been identified for patient 1, we showed that these markers of $CD8^+$ T-cell activation were also severely impaired against HLA-matched EBV-B cells. Importantly, addition of 4-1BB inhibitory antibody to normal PBMCs stimulated with allogeneic or autologous EBV-B cells reduced $CD8^+$ T-cell expansion, expression of IFN-γ and perforin, and cytotoxicity to levels comparable with those in the patients, thus recapitulating the functional defects of the patient's $CD8^+$ T cells. These findings also replicate defects in the expansion, IFN-γ production, and function of allocytotoxic $CD8^+$ T cells from 4-1BB–deficient mice.[21]

Costimulatory molecules, such as CD28 and inducible costimulator, have been shown to enhance mitochondrial respiration, biogenesis, and increased membrane potential.[34] Mitochondrial function is critical for the function of activated T cells.[35] Activated $CD8^+$ T cells from the patients showed decreased oxygen consumption, decreased mitochondrial mass, and reduced membrane potential. These defects are consistent with the known contribution of 4-1BB stimulation in promoting mitochondrial respiration and biogenesis[20] and likely contribute to the defective cytotoxicity of the patients' $CD8^+$ T cells against allogeneic and HLA-matched EBV-B cell targets. This is relevant to the patients' inability in clearing EBV infections and the failure of patient 2 to eliminate his EBV-triggered B-cell lymphoma.

NK cells, like T cells, express 4-1BB on their activation through incubation with their targets and cytokines (IL-2, IL-15, or IL-21).[36] Also, like in T cells, 4-1BB signaling promotes proliferation and IFN-γ secretion by activated NK cells.[12] However, the effect of 4-1BB ligation on the cytotoxicity of activated NK cells is controversial, with some studies showing enhancement and others showing inhibition.[37-39] Given the ethical limitations on repeated blood sampling from patients with complex medical disorders, future studies with additional patients will be needed to define the role of 4-1BB on NK cytotoxicity.

Although the 2 patients we studied were from unrelated families, they shared a single ROH, suggesting a founder effect. *TNFRSF9* was the only one of the 2 genes in the shared ROH that had a novel variant and was predicted to be pathogenic. Furthermore, the $CD8^+$ T-cell defects in both patients were similar to those in *Tnfrsf9*$^{-/-}$ mice. Together, these findings implicate the lack of 4-1BB expression as the cause of the disease in our patients. Identification of different mutations in *TNFRSF9* in patients with EBV-driven lymphoproliferation will provide further support for a causative role of 4-1BB deficiency.

In summary, we have identified a novel immunodeficiency associated with EBV lymphoproliferation caused by a homozygous mutation in 4-1BB. Our results indicate the clinical importance of 4-1BB in immune surveillance against infection with EBV and its complications.

We are grateful to the patients and the patients' families for their participation in this study. We thank Dr Klaus Schwarz for facilitating the study. We thank the Genotyping and Sequencing Core Facilities at KFSHRC for their technical help.

Key messages

- **We identified a homozygous missense mutation in TNFRSF9 encoding the T-cell costimulatory molecule 4-1BB in 2 unrelated patients with recurrent infections, persistent EBV viremia, and EBV-induced lymphoproliferation.**
- **The 4-1BB mutation abolished surface expression of 4-1BB on activated T cells.**
- **$CD8^+$ T cells from the patients had impaired proliferation, reduced expression of IFN-γ and perforin, and diminished cytotoxic activity in response to stimulation with allogeneic and HLA-matched EBV-transformed B cells.**
- **Activated $CD8^+$ T cells from the patients had reduced mitochondrial mass, membrane potential, and function.**

REFERENCES

1. Kurth J, Spieker T, Wustrow J, Strickler GJ, Hansmann LM, Rajewsky K, et al. EBV-infected B cells in infectious mononucleosis: viral strategies for spreading in the B cell compartment and establishing latency. Immunity 2000;13:485-95.
2. Latour S, Winter S. Inherited immunodeficiencies with high predisposition to Epstein-Barr virus-driven lymphoproliferative diseases. Front Immunol 2018;9:1103.
3. Palendira U, Rickinson AB. Primary immunodeficiencies and the control of Epstein-Barr virus infection. Ann N Y Acad Sci 2015;1356:22-44.
4. Katano H, Ali MA, Patera AC, Catalfamo M, Jaffe ES, Kimura H, et al. Chronic active Epstein-Barr virus infection associated with mutations in perforin that impair its maturation. Blood 2004;103:1244-52.
5. Yamada S, Shinozaki K, Agematsu K. Involvement of CD27/CD70 interactions in antigen-specific cytotoxic T-lymphocyte (CTL) activity by perforin-mediated cytotoxicity. Clin Exp Immunol 2002;130:424-30.
6. van Montfrans JM, Hoepelman AI, Otto S, van Gijn M, van de Corput L, de Weger RA, et al. CD27 deficiency is associated with combined immunodeficiency and persistent symptomatic EBV viremia. J Allergy Clin Immunol 2012;129:787-93.e6.
7. Izawa K, Martin E, Soudais C, Bruneau J, Boutboul D, Rodriguez R, et al. Inherited CD70 deficiency in humans reveals a critical role for the CD70-CD27 pathway in immunity to Epstein-Barr virus infection. J Exp Med 2017;214:73-89.
8. Abolhassani H, Edwards ES, Ikinciogullari A, Jing H, Borte S, Buggert M, et al. Combined immunodeficiency and Epstein-Barr virus-induced B cell malignancy in humans with inherited CD70 deficiency. J Exp Med 2017;214:91-106.
9. Bitra A, Doukov T, Croft M, Zajonc DM. Crystal structures of the human 4-1BB receptor bound to its ligand 4-1BBL reveal covalent receptor dimerization as a potential signaling amplifier. J Biol Chem 2018;293:9958-69.
10. Jang IK, Lee ZH, Kim YJ, Kim SH, Kwon BS. Human 4-1BB (CD137) signals are mediated by TRAF2 and activate nuclear factor-kappa B. Biochem Biophys Res Commun 1998;242:613-20.

11. Harfuddin Z, Kwajah S, Chong Nyi Sim A, Macary PA, Schwarz H. CD137L-stimulated dendritic cells are more potent than conventional dendritic cells at eliciting cytotoxic T-cell responses. Oncoimmunology 2013;2:e26859.
12. Wilcox RA, Tamada K, Strome SE, Chen L. Signaling through NK cell-associated CD137 promotes both helper function for CD8+ cytolytic T cells and responsiveness to IL-2 but not cytolytic activity. J Immunol 2002;169:4230-6.
13. Watts TH. TNF/TNFR family members in costimulation of T cell responses. Annu Rev Immunol 2005;23:23-68.
14. Stephan MT, Ponomarev V, Brentjens RJ, Chang AH, Dobrenkov KV, Heller G, et al. T cell-encoded CD80 and 4-1BBL induce auto- and transcostimulation, resulting in potent tumor rejection. Nat Med 2007;13:1440-9.
15. Choi IK, Wang Z, Ke Q, Hong M, Qian Y, Zhao X, et al. Signaling by the Epstein-Barr virus LMP1 protein induces potent cytotoxic CD4(+) and CD8(+) T cell responses. Proc Natl Acad Sci U S A 2018;115:E686-95.
16. Laderach D, Movassagh M, Johnson A, Mittler RS, Galy A. 4-1BB co-stimulation enhances human CD8(+) T cell priming by augmenting the proliferation and survival of effector CD8(+) T cells. Int Immunol 2002;14:1155-67.
17. Shuford WW, Klussman K, Tritchler DD, Loo DT, Chalupny J, Siadak AW, et al. 4-1BB costimulatory signals preferentially induce CD8+ T cell proliferation and lead to the amplification in vivo of cytotoxic T cell responses. J Exp Med 1997;186:47-55.
18. Wen T, Bukczynski J, Watts TH. 4-1BB ligand-mediated costimulation of human T cells induces CD4 and CD8 T cell expansion, cytokine production, and the development of cytolytic effector function. J Immunol 2002;168:4897-906.
19. Menk AV, Scharping NE, Rivadeneira DB, Calderon MJ, Watson MJ, Dunstane D, et al. 4-1BB costimulation induces T cell mitochondrial function and biogenesis enabling cancer immunotherapeutic responses. J Exp Med 2018;215:1091-100.
20. Teijeira A, Labiano S, Garasa S, Etxeberria I, Santamaria E, Rouzaut A, et al. Mitochondrial morphological and functional reprogramming following CD137 (4-1BB) costimulation. Cancer Immunol Res 2018;6:798-811.
21. Kwon BS, Hurtado JC, Lee ZH, Kwack KB, Seo SK, Choi BK, et al. Immune responses in 4-1BB (CD137)-deficient mice. J Immunol 2002;168:5483-90.
22. Bartkowiak T, Curran MA. 4-1BB agonists: multi-potent potentiators of tumor immunity. Front Oncol 2015;5:117.
23. Chester C, Ambulkar S, Kohrt HE. 4-1BB agonism: adding the accelerator to cancer immunotherapy. Cancer Immunol Immunother 2016;65:1243-8.
24. Chester C, Sanmamed MF, Wang J, Melero I. Immunotherapy targeting 4-1BB: mechanistic rationale, clinical results, and future strategies. Blood 2018;131:49-57.
25. Li G, Boucher JC, Kotani H, Park K, Zhang Y, Shrestha B, et al. 4-1BB enhancement of CAR T function requires NF-kappaB and TRAFs. JCI Insight 2018;3.
26. Monies D, Abouelhoda M, AlSayed M, Alhassnan Z, Alotaibi M, Kayyali H, et al. The landscape of genetic diseases in Saudi Arabia based on the first 1000 diagnostic panels and exomes. Hum Genet 2017;136:921-39.
27. Alkuraya FS. Discovery of mutations for Mendelian disorders. Hum Genet 2016;135:615-23.
28. Jabara HH, Boyden SE, Chou J, Ramesh N, Massaad MJ, Benson H, et al. A missense mutation in TFRC, encoding transferrin receptor 1, causes combined immunodeficiency. Nat Genet 2016;48:74-8.
29. Hui-Yuen J, McAllister S, Koganti S, Hill E, Bhaduri-McIntosh S. Establishment of Epstein-Barr virus growth-transformed lymphoblastoid cell lines. J Vis Exp 2011;57.
30. Noto A, Ngauv P, Trautmann L. Cell-based flow cytometry assay to measure cytotoxic activity. J Vis Exp 2013;82:e51105.
31. Chacon JA, Wu RC, Sukhumalchandra P, Molldrem JJ, Sarnaik A, Pilon-Thomas S, et al. Co-stimulation through 4-1BB/CD137 improves the expansion and function of CD8(+) melanoma tumor-infiltrating lymphocytes for adoptive T-cell therapy. PLoS One 2013;8:e60031.
32. Zhang X, Voskens CJ, Sallin M, Maniar A, Montes CL, Zhang Y, et al. CD137 promotes proliferation and survival of human B cells. J Immunol 2010;184:787-95.
33. Ryffel B, Di Padova F, Schreier MH, Le Hir M, Eugster HP, Quesniaux VF. Lack of type 2 T cell-independent B cell responses and defect in isotype switching in TNF-lymphotoxin alpha-deficient mice. J Immunol 1997;158:2126-33.
34. Klein Geltink RI, O'Sullivan D, Corrado M, Bremser A, Buck MD, Buescher JM, et al. Mitochondrial priming by CD28. Cell 2017;171:385-97.e11.
35. Sena LA, Li S, Jairaman A, Prakriya M, Ezponda T, Hildeman DA, et al. Mitochondria are required for antigen-specific T cell activation through reactive oxygen species signaling. Immunity 2013;38:225-36.
36. Li X, He C, Liu C, Ma J, Ma P, Cui H, et al. Expansion of NK cells from PBMCs using immobilized 4-1BBL and interleukin-21. Int J Oncol 2015;47:335-42.
37. Vinay DS, Choi BK, Bae JS, Kim WY, Gebhardt BM, Kwon BS. CD137-deficient mice have reduced NK/NKT cell numbers and function, are resistant to lipopolysaccharide-induced shock syndromes, and have lower IL-4 responses. J Immunol 2004;173:4218-29.
38. Baessler T, Charton JE, Schmiedel BJ, Grunebach F, Krusch M, Wacker A, et al. CD137 ligand mediates opposite effects in human and mouse NK cells and impairs NK-cell reactivity against human acute myeloid leukemia cells. Blood 2010;115:3058-69.
39. Navabi S, Doroudchi M, Tashnizi AH, Habibagahi M. Natural killer cell functional activity after 4-1BB costimulation. Inflammation 2015;38:1181-90.

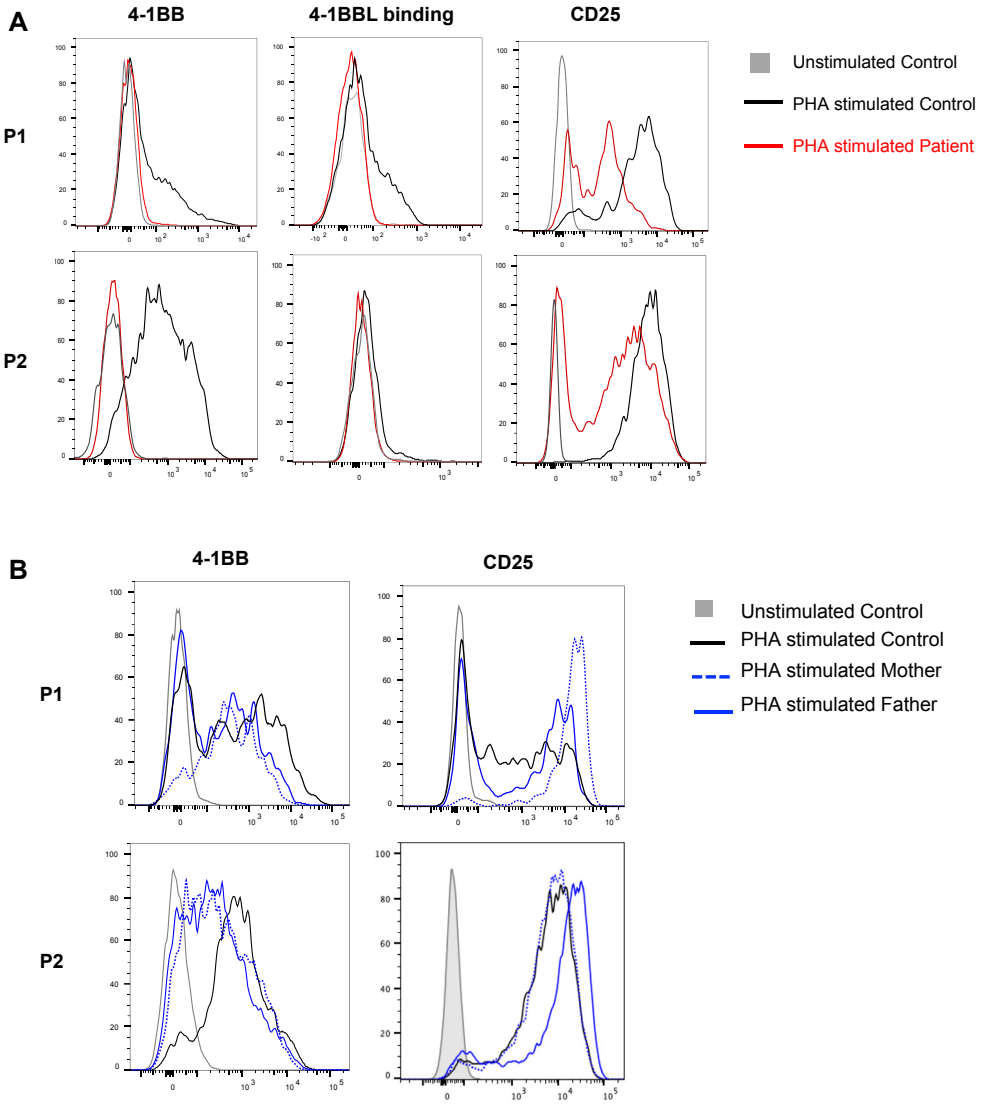

FIG E1. Effect of the 4-1BB^{G109S} mutation on 4-1BB surface expression by activated CD4^{+} T cells from the patients and activated CD8^{+} T cells from the parents. **A,** Fluorescence-activated cell-sorting analysis of 4-1BB expression *(left panels)*, 4-1BBL binding *(center panels)*, and CD25 expression *(right panels)* in PHA-stimulated CD4^{+} T cells from the patients and control subjects. Similar results were obtained from 2 independent experiments. **B,** Fluorescence-activated cell-sorting analysis of 4-1BB expression *(left)* and CD25 expression *(right)* in PHA-stimulated CD8^{+} T cells from the patients' parents and a control subject.

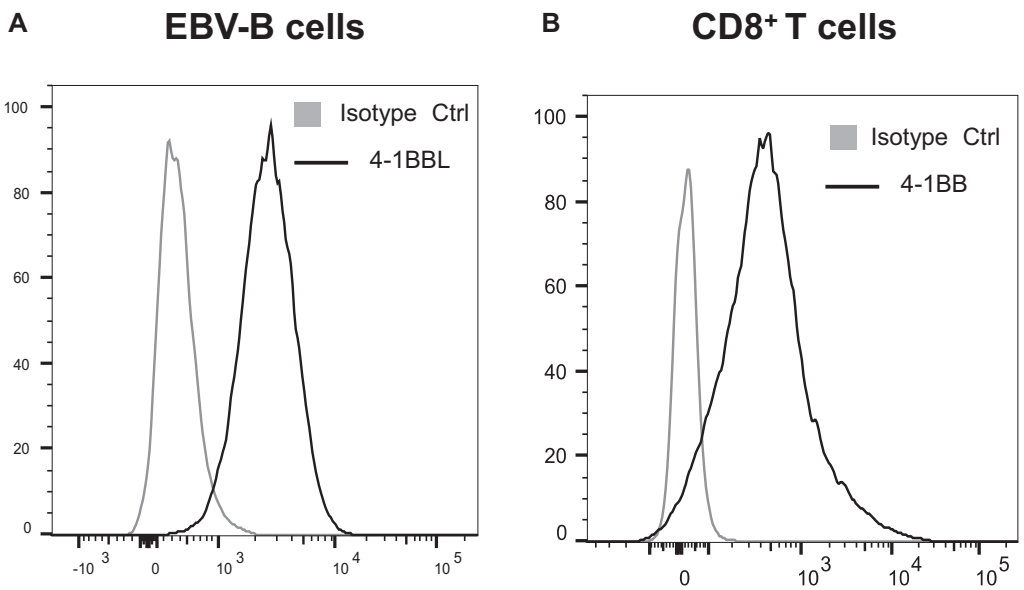

FIG E2. Expression of 4-1BBL on EBV-B cells and 4-1BB on $CD8^+$ T cells in cultures of normal PBMCs stimulated with allogeneic B cells. Representative fluorescence-activated cell-sorting analysis of 4-1BBL expression on EBV-B cells **(A)** and 4-1BB expression on $CD8^+$ T cells examined on day 14 of stimulation with allogeneic EBV-B cells **(B)** is shown. *Gray profiles* represent staining with isotype control *(Ctrl.)*. Similar results were obtained from 2 independent experiments.

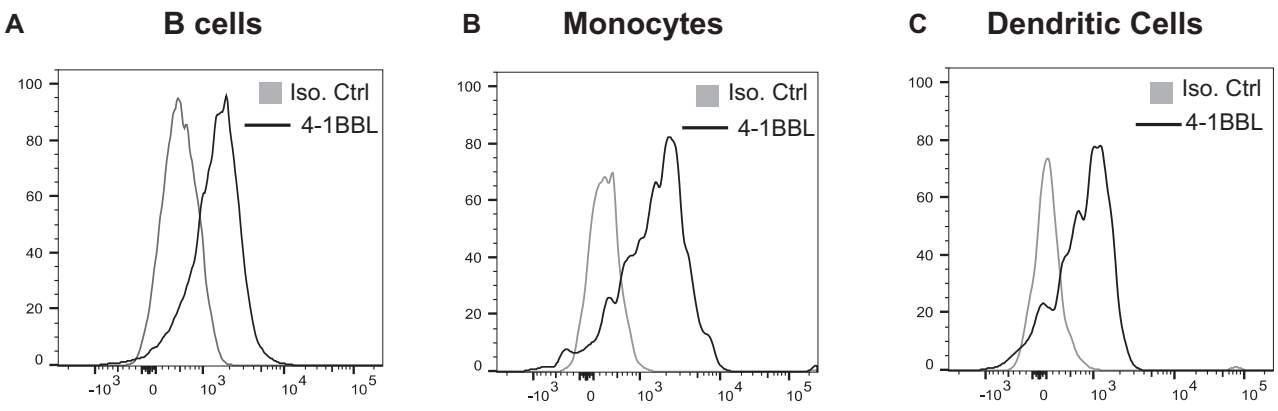

FIG E3. Expression of 4-1BBL in PHA-stimulated cultures of normal PBMCs. Representative fluorescence-activated cell-sorting analysis of 4-1BBL expression on $CD19^+$ B cells **(A)**, $CD14^+$ monocytes **(B)**, and $CD11c^+$ dendritic cells **(C)** in PHA cultures is shown. *Gray profiles* represent staining with isotype control *(Iso. Ctrl.)* is shown. Similar results were obtained from 2 independent experiments.

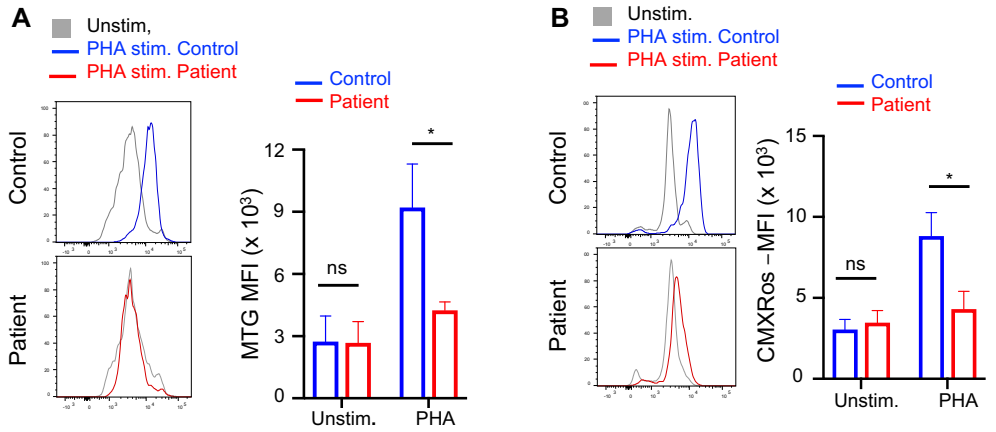

FIG E4. Defective mitochondrial biogenesis and function in patients' activated $CD4^+$ T cells. Representative fluorescence-activated cell-sorting analysis *(left)* and quantitative analysis (mean fluorescence intensity *[MFI]*, *right*) of mitochondrial mass measured by using MitoTracker Green (*MTG*; **A**) and mitochondrial membrane potential measured by using MitoTracker Red CMXRos **(B)** of $CD4^+$ cells from PHA-stimulated cultures of PBMCs from patients (n = 2) and control subjects (n = 3) is shown. *Columns* and *bars* represent means + SEMs. $*P < .05$ and $**P < .01$. *ns*, Not significant.

TABLE E1. Variants shared by both probands with a minor allele frequency of less than 0.001 in gnomAD

Chromosome	Position	Gene name	Zygosity	Variants
2	133075726	*ZNF806*	Heterozygous	NM_001304449: c.1187A>G:p.Glu396Gly
2	133075904	*ZNF806*	Heterozygous	NM_001304449: c.1366dupA:p.Asn456Lysfs*85
3	42251580	*TRAK1*	Heterozygous	NM_001265608: c.2064_2066del:p.Glu698del
9	140773612	*CACNA1B*	Heterozygous	NM_000718: c.390+1->ACGACACGGAGCCCTATTTCATCGGG ATCTTTTGCTTCGAGGCAGGGA
17	21318588	*KCNJ12*	Heterozygous	NM_021012: UTR5.c.-65C>G
17	9000169	*MUC16*	Heterozygous	NM_024690: c.40588G>A:p.Gly13530Ser
1	7998274	*TNFRSF9*	Homozygous	NM_001561: c.325G>A:p.Gly109Ser
1	7724977	*CAMTA1*	Homozygous	NM_015215: c.2370C>G:p.Ile790Met